

Form Approved
OMB No. 0704-0188

3. DATES COVERED (From - To)

Paper

5a. CONTRACT NUMBER**5b. GRANT NUMBER****5c. PROGRAM ELEMENT NUMBER****5d. PROJECT NUMBER**

2302

5e. TASK NUMBER

M1G2

5f. WORK UNIT NUMBER

8. PERFORMING ORGANIZATION REPORT

AFRL-PR-ED-TP-2000-001

10. SPONSOR/MONITOR'S ACRONYM(S)

11. SPONSOR/MONITOR'S
NUMBER(S)

AFRL-PR-ED-TP-2000-001

12. DISTRIBUTION / AVAILABILITY STATEMENT
Approved for public release; distribution unlimited.

13. SUPPLEMENTARY NOTES

14. ABSTRACT

20020115 094

15. SUBJECT TERMS

17. LIMITATION OF ABSTRACT

18. NUMBER OF PAGES

19a. NAME OF RESPONSIBLE PERSON

c. THIS PAGE
Unclassified

A

19b. TELEPHONE NUMBER
(include area code)
(661) 275-5642

EFFECT OF LOAD HISTORY ON DAMAGE CHARACTERISTICS NEAR CRACK TIPS IN A PARTICULATE COMPOSITE MATERIAL

C.T. LIU

Air Force Research Laboratory
AFRL/PRSM
10 E. Saturn Blvd.
Edwards AFB CA 93524-7680

ABSTRACT

The damage field in a precracked particulate composite specimen subjected to a complex cyclic loading history was investigated using acoustic imaging techniques. The acoustic imaging data were analyzed to delineate the damage field ahead of the crack tips and to generate contour plots of the damage intensity. The results of these analyses were compared and the effect of the loading history on the damage field is discussed.

INTRODUCTION

On the microscopic scale a highly filled polymeric material can be considered nonhomogeneous. When this material is stretched, the different sizes and the distribution of the filler particles, the different crosslink density of polymer chains, and the variation of bond strengths between the particles and the binder can produce high nonhomogeneous local stress and strength fields. When this material is strained, depending on the magnitudes of the local stress and strength, damage may develop in the material. The damage may be in the form of microvoids or microcracks in the binder or in the form of dewetting between the binder and the filler particles. Since the local stress and strength vary in a random fashion, the damage will not be confined to a specific location. Instead it will diffuse into a relatively larger area or zone. The growth of damage in the material may occur by material tearing or by successive nucleation and coalescence of the microvoids. These time-dependent cumulative damage processes are the main factor responsible for the time sensitivity of the strength degradation as well as the fracture behavior of particle-filled polymeric materials, such as solid propellants. Therefore, to gain an advanced understanding of fracture behavior of solid propellant, detailed knowledge of the characteristics of damage initiation and evolution is required.

In the past, acoustic imaging techniques were used to determine the damage field near the crack tips in

particulate composites⁽¹⁻⁴⁾. Experimental results indicated that extensive damage (microcracks and microvoids) occurred near the crack tip and, initially, the damage zone's shape was very similar to the plastic zone's shape near the crack tip in metals. It was found that damage zone size and intensity were highly dependent on load history. In addition, a comparison of results of finite element analysis revealed that damage distribution was roughly commensurate with the stress distribution in the specimen.

In this study, the characteristics of damage field in a particulate composite material, containing hard particles embedded in a rubbery matrix, subjected to a complex load history were investigated using a 7.62 cm x 7.26 cm x 0.508 cm (3 in x 2.5 in x 0.2 in) pre-cracked sheet specimen. A razor blade was used to cut three 2.54 cm (1.0 in) cracks, one at the center and two near the edges of the specimen, through the thickness of the specimen. The three cuts were parallel to the longest side of the specimen and perpendicular to the loading direction. During the test, Lockheed Research Laboratory's acoustic-imaging system was used to determine the characteristics of the damage field in the specimen. The results of these analyses were compared and the effect of loading history on damage characteristics is discussed.

SPECIMEN AND TESTING

The effect of cyclic loading on the cumulative damage in a particulate composite material was investigated using a pre-cracked specimen. The geometry of the pre-cracked specimen with three 2.54 cm (1.0 in) cracks is shown in Fig. 1. During the cyclic strain test, the strain cycle had a triangular shape with a minimum strain level of 0%, and a maximum strain level of 6%. Fig. 2 is a schematic representation of the cyclic loading.

In this study Lockheed Research Laboratory's acoustic-imaging system was used to measure the transmitted acoustic energy in a scanning mode. Because acoustic imaging is conveniently performed in a water tank, a Lucite container was constructed to hold the glycerol fluid in which a straining device could be immersed. The container was immersed in a water tank. During the test, the acoustic wave with a wavelength short enough to exhibit quasi-optical behavior was radiated from an insonifier combined with a plane-concave polystyrene lens, which focused acoustic energy at a desired location in the material to be studied. Acoustic energy passing through the material was

recovered by a receiver lens of similar geometry and configuration, which transmitted the acoustic energy to a receiving transducer. The receiving transducer converted the transmitted acoustic energy into a corresponding electrical signal which was stored in a computer for further data analysis.

A two-dimensional acoustic image is generated in a common focal plane of the lenses by mechanical translation of the two lens/transducer units together in a plan normal to the acoustic transmission path. Each translation generates one scan line in the image. After each scan has been completed, the scan mechanism steps one unit in evaluation, and another line scan is performed. Approximately 512 data points are generated per scan line, and 100 lines are scanned per inch of test material. An ultrasonic frequency of 1.9 MHz is used in the test. A detailed description of the testing setup and some of the basic components used in the acoustic imaging system can be found in Reference 1.

Recorded experimental data were processed to create a visual representation of the energy absorbed in the material being inspected. A region of high ultrasonic absorption, i.e., a highly damaged area, will be shown as a dark area and a region of unattenuated ultrasonic wave will produce a light or white area with 254 shades of gray in between. The acoustic image at a given strain level was plotted in the form of iso-intensity contours of the transmitted acoustic energy to enhance the resolution of the damage field.

RESULTS AND DISCUSSION

Typical acoustic images of the specimen at different strain levels of the first strain cycle are shown in Fig. 3. The virgin specimen's dappled appearance, as revealed in its acoustic image, was its prominent feature. The dappled appearance may have been caused by a number of factors such as the existence of a cluster of filler particles in a small region, undercure of the binder material in a local area, and large voids in the material. The dappled appearance is also an indication of the material's nonhomogeneity. When the specimen is strained, the high intensity of stress near the crack tip will induce higher damage in the material. As the material is damaged, the acoustic energy transmitted through the damaged region will be attenuated, or the intensity of the transmitted energy, I_t , will decrease, resulting in a dark area near the crack tip (Figs. 3b and 3c). The size of the dark area or the size of the

damage zone increases with increasing strain level. To delineate the damage zone, the acoustic data were analyzed and contours of iso-intensity of I_t were plotted.

Plots of iso-intensity contours of I_t as a function of the applied strain are shown in Fig. 4. In Fig. 4, the number between two contour lines is the range of I_t between the prior and the next intensity levels. A small number indicates that the intensity of the transmitted acoustic energy is low or the damage is high. These contour plots reveal that the size of the damage zone and the intensity of damage increased as the strain level increased. This phenomenon, under a monotonically-increasing loading condition, was expected because the magnitude of the stress increased due to the increased applied strain level. Consequently, the severity of damage and the size of the damage zone increased. Fig. 4 also reveals that a large increase in damage zone size and intensity of damage in the damage zone occurred near the crack tip as the applied strain increased. However, damage intensities in the two center regions between the cracks slightly increased as applied stress was increased from 0% to 6%. This occurred because the magnitudes of the stress in the two center regions between the cracks were relatively small. In other words, the existence of the cracks produced a "shielding" effect on the material in the two center regions of the specimen. Referring back to Fig. 4, it is seen that the damage distributions are not symmetrical with respect to the vertical and horizontal center lines of the specimen and the crack planes. This is another indication of the nonhomogeneous nature of the microstructure. It is interesting to point out that the effect of microstructure on damage distribution depends on the applied strain level. At a small applied strain level, the microstructure of the material has a relatively large effect on the damage distribution, whereas at a higher applied strain level, the damage distributions are relatively symmetrical with respect to the crack planes as shown in Fig. 4. From Fig. 4, we also note that the crack opening displacements, COD, for the three cracks are different. The center crack had the largest COD; the lower crack had the smallest COD. This is consistent with the stress analysis results which indicated that the value of the Mode I stress intensity factor at the tip of the center crack was larger than that near the upper crack tip which, in turn, is slightly larger than that near the lower crack tip. It should be pointed out that because of acoustic noise, the size of the apparent crack in Fig. 3 is relatively larger than the actual crack.

In the following paragraphs, the effect of load history on the damage characteristics in the specimen is discussed.

According to the applied strain history shown in Fig. 2, 6% strain was applied to the specimen for one hour. Then the strain was unloaded to 0% strain and held at 0% strain for three hours. Two images were taken during the hour that 6% strain was applied, and Also, two images were taken during the three hours that 0% strain was applied. For both cases, one image was taken at the beginning of the time period; the other taken at the end of the time period.

The iso-intensity contour plots of I_t near the right side tip of the center crack while the specimen was held at 6% strain and 0% strain are shown in Fig. 5a and Fig. 5b, respectively. A comparison of the iso-intensity contour plots of I_t shown in Fig. 5a reveals that a slight change in the contour plots of I_t occurred near the crack tip while the specimen was held at 6% strain for 1 hour. The increase in the low damage intensity zone sizes, for example for I_t equal to 40, is believed to be due to the decrease in void size as a result of stress relaxation under constant applied strain condition. The acoustic data also show that, although stress is relaxed under constant strain, the size and distribution of the microvoids did not change significantly as long as the specimen was stretched. In other words, the material's microstructure and damage characteristics did not change much. However, when the specimen was relaxed during the 3-hour 0% strain cycle, the acoustic imaging data show very different results as shown in Fig. 5b. This indicates that the strain level applied to the specimen for a long time can have a significant effect on the measured damage intensity and damage zone size.

In Fig. 5b, we note that the damage regions still exist when the specimen is imaged immediately after the specimen is unloaded to 0% strain. This indicates that although the applied strain is zero at the end of the first strain cycle, local microstrain between particles in the damage regions, especially in the highly damaged regions near the crack tips, is not zero. The existence of tensile residual strain will prevent microvoids and microcracks, generated by the previously applied strain, from closing. As time elapses, microvoid size will decrease due to the time-dependent nature of the material's deformation process. In addition, the existence of damage regions immediately after the specimen is unloaded to 0% strain probably due to the fact that the local material response lagged behind the applied load. In other words, because of the material's viscoelastic nature, there is a time scale or phase shift⁽⁵⁾ and that it takes time to rearrange the microstructure, such as the movement of filler particles in the material to respond to

applied load. The decrease in microvoid size with increasing time should be manifested by the increase in I_t value. In other words, damage zone size as well as damage intensity will decrease as the length of time increases. This time dependence of damage characteristics is clearly shown in Fig. 5b.

The iso-intensity contours of I_t at 3% strain and 6% strain of the unloading branch of the first strain cycle and the loading branch of the second and the third strain cycles are shown in Fig. 6. Comparing Fig. 6a with Figs. 6b and 6c shows that the damage zone's size and shape as well as the intensity of damage measured at the two strain levels of the unloading branch of the first strain cycle are significantly different from that measured at the two strain levels of the loading branch of other strain cycles. This indicates that the first strain cycle has a significant effect on the damage developed in the material. The effects of applying 10 small amplitude strain cycles, which has a maximum strain of 3%, on the damage characteristics are shown in Fig. 7. It is interesting to note that the damage characteristics depend on the applied strain level at which the acoustic image was taken. At 0% applied strain level, Figs. 7a and 7b show that the sizes of the damage zones are reduced; this indicates that instead of increasing the amount of damage, the 10 small strain cycles reduced the severity of the damage near the crack tip. This phenomenon is believed to be related to the development of the residual compressive stress at the end of each strain cycle. The development of compressive stress under cyclic loading condition was reported by Liu⁶ in his study of the effect of cyclic loading sequence on cumulative damage and constitutive behavior in a composite solid propellant. It was found that the compressive stress depends on the maximum strain of the strain cycles; the higher the maximum cyclic strain, the higher the compressive stress. It was also found that the relative attenuation of ultrasonic wave, which is related to damage in the material, is reduced as a result of the development of compressive stress. Similarly, by comparing the damage characteristics at 6% applied strain level of the second and third strain cycle reveals that the application of 10 small amplitude strain cycles reduces damage severity near the crack tip.

In this study, in addition to plotting the iso-intensity contours of I_t , the profiles of I_t along the specimen's vertical plane of symmetry were also plotted, and typical profile plots are shown in Fig. 8. By examining Fig. 8, the effect of load history on the damage characteristics in the "shielding" regions between the cracks can be determined. Figure 8a shows the profiles of I_t at 0% strain for the virgin specimen and for the specimen before and

after it is subjected to the 10 small amplitude strain cycles. Figure 8b shows the profiles of I_t at 6% strain of the first and third strain cycles. It is interesting to note that the values of I_t increase as the strain cycle is increased. The increase in I_t or decrease in damage is believed to be due to the effect of compressive stress developed at the end of each strain cycles as discussed previously.

CONCLUSIONS

The acoustic imaging data presented in this paper show that load history has a significant effect on damage zone size and damage intensity in particulate composites. The dependence of damage characteristics on the load history is believed to be related to the results of the complex interaction among the residual stress field, the residual strain fields, cumulative damage, and time-dependent nature of the matrix material. Since the current damage state depends on past load history, exercise caution when interpreting either acoustic imaging results or other nondestructive testing results.

Although nondestructive testing techniques can be used to detect damage in particulate composites, interpreting results in terms of physical damage parameters and evaluating the effect of damage state on crack growth behavior are problematic at this time. It is recommended that development of nondestructive testing techniques for damage detection and interpretation of test results proceed in a fashion which emphasizes concurrent investigation of nondestructive test methods and damage mechanics. Only by understanding both the effect of damage on a material's response and the nondestructive test methods can we hope to develop the required nondestructive test techniques.

REFERENCES

1. Martinson, R.H., and Hartog, J.J., "Acoustic Imaging Applied to Crack Propagation Studies", 16th JANNAF Structures and Mechanical Behavior Subcommittee Meeting, CPIA Publication 311, Volume I, March 1980, pp.

2. Liu, C.T., and Yee, R., "Evaluation of Cumulative Damage in a Composite Solid Propellant", Proceedings of the 1986 Society for Experimental Mechanics Conference on Experimental Mechanics held June 8-13, 1986 in New Orleans, LA.
3. Liu, C.T., "Investigating the Damage Field Near Crack Tips in a Composite Solid Propellant", Proceedings of the 1987 Society for Experimental Mechanics Conference on Experimental Mechanics held June 14-19, 1987 in Houston, TX.
4. Liu, C.T., "The Measurement of Damage in a Solid Propellant by Acoustic Imaging Technique", AIAA/SAE/ASME/SAE 23rd Joint Propulsion Conference held June 29-July 2, 1987 in San Diego, CA.
5. Smith, G.C., Palaniswamy, K., and Knauss, W.C., The Application of Rate Theory to the Failure of Solid Propellants, AFRPL-TR-73-54, Graduate Aeronautical Laboratories, California Institute of Technology, Pasadena, CA, July 1973.
6. Liu, C.T., "Effects of Cyclic Loading Sequence on Cumulative Damage and Constitutive Behavior of a Composite Solid Propellant", AIAA/ASME/ASME/SAE 28th Structures, Structural Dynamics, and Materials Conference held April 6, 1987 in Monterey, CA.

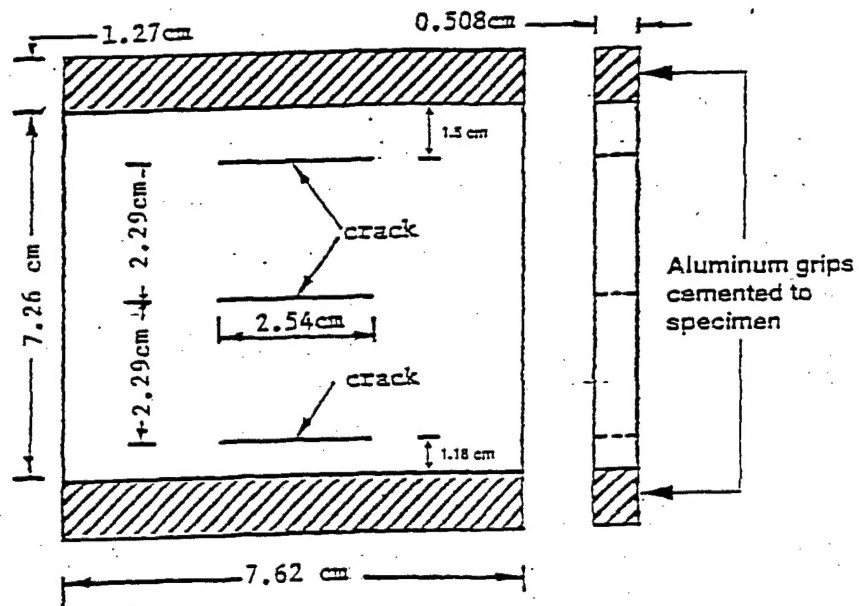


Fig. 1. Specimen geometry.

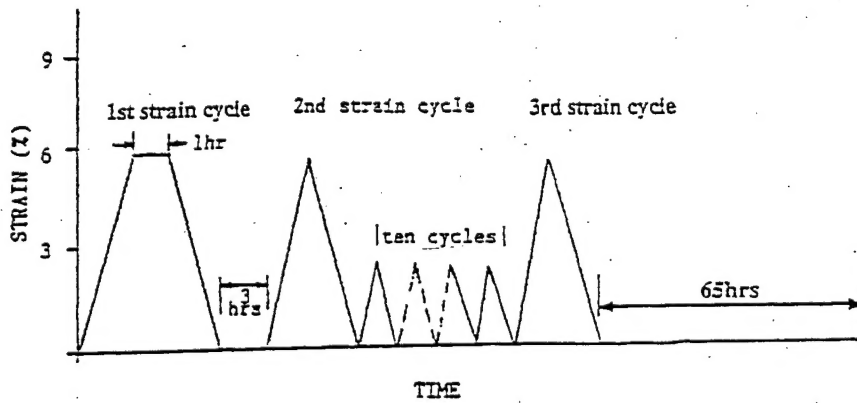
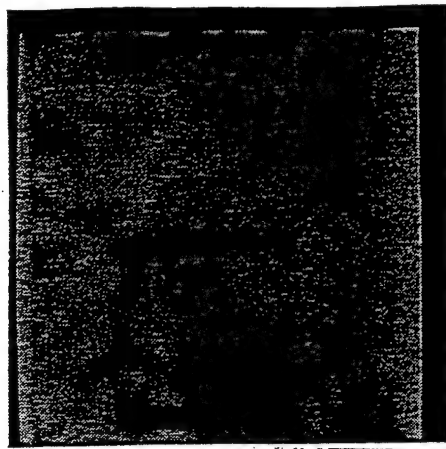


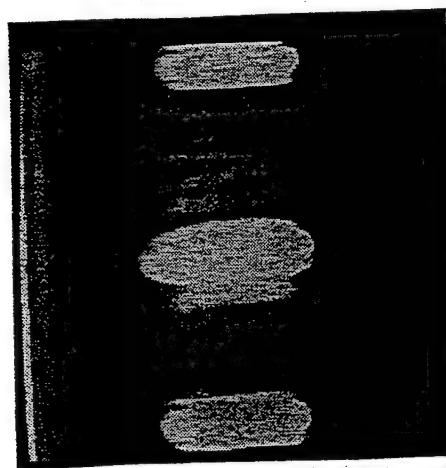
Fig. 2. Schematic representation of cyclic loading.



(a) 0% applied strain

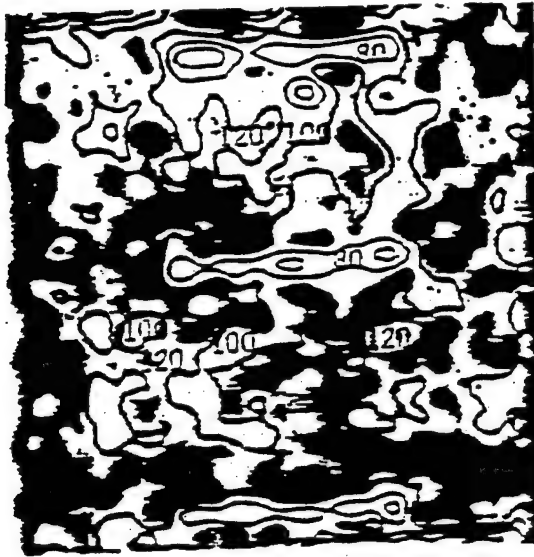


(b) 3% applied strain



(c) 6% applied strain

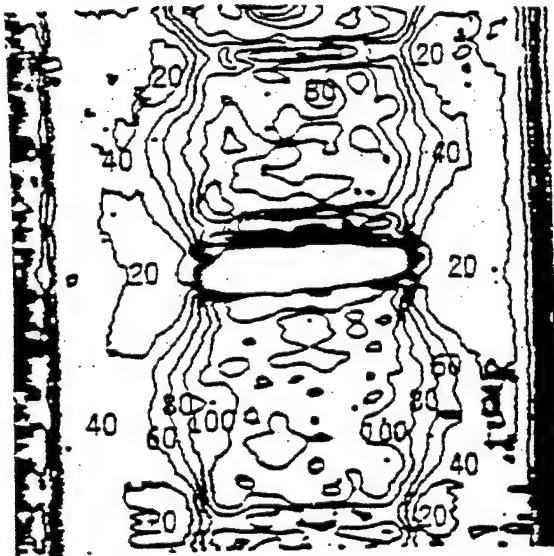
Fig. 3. Acoustic images of the specimen for the loading branch of the first strain cycle



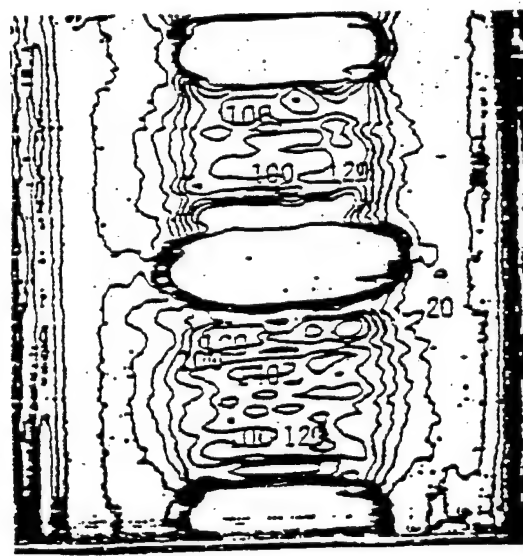
(a) 0% applied strain (loading)



(b) 3% applied strain (loading)

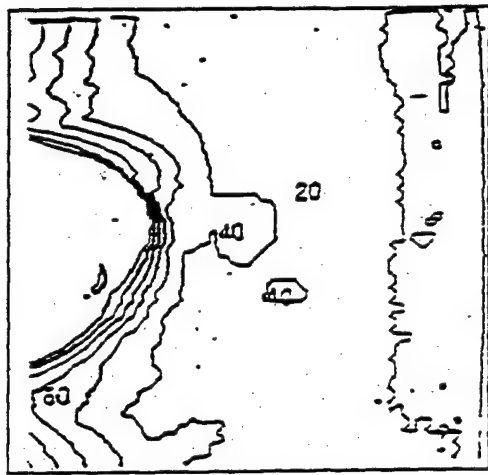


(d) 3% applied strain (unloading)

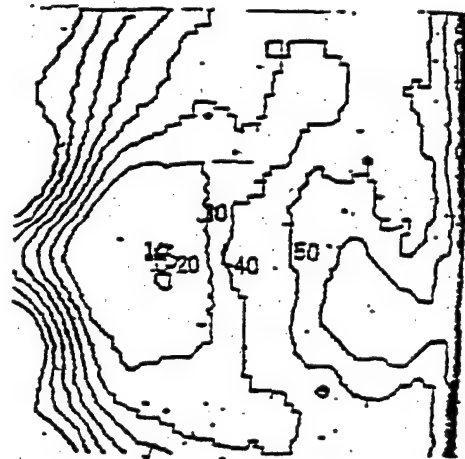


(c) 6% applied strain (loading)

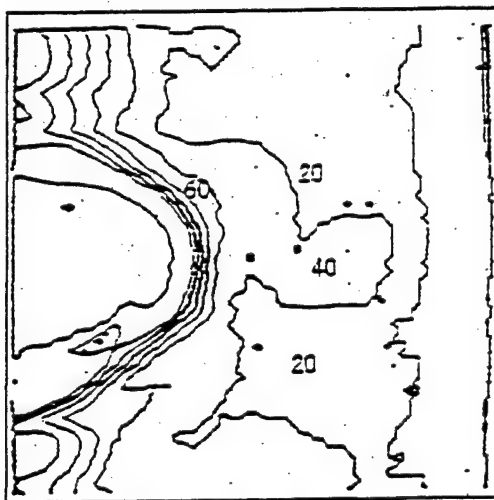
Fig.4. Iso-intensity contour plots of acoustic images of the specimen
(first strain cycle)



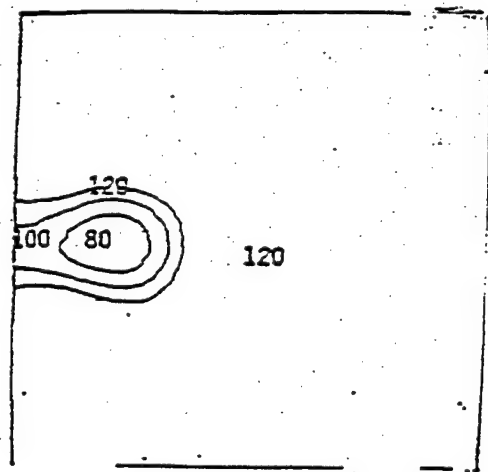
AT THE BEGINNING OF THE ONE HOUR PERIOD



AT THE BEGINNING OF THE THREE HOUR PERIOD



AT THE END OF THE ONE HOUR PERIOD

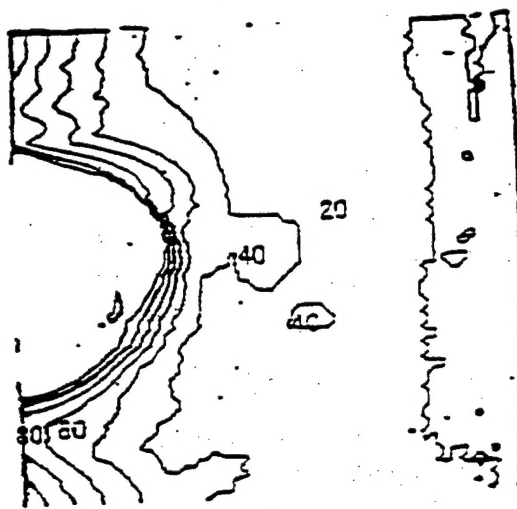


AT THE END OF THE THREE HOUR PERIOD

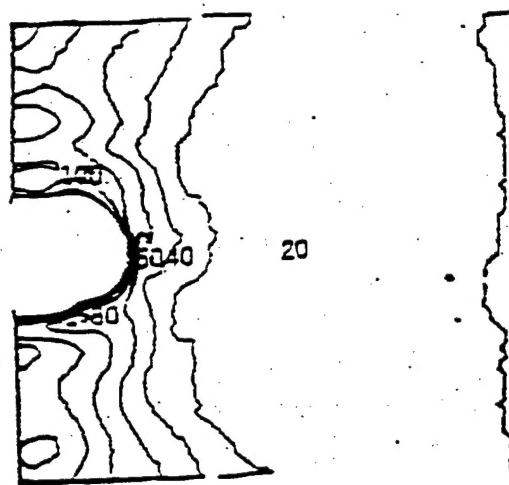
(a) 6% applied strain

(b) 0% applied strain

Fig. 5. Iso-intensity contour plots of acoustic images near the tip of the center crack (6% applied strain and 0% applied strain)

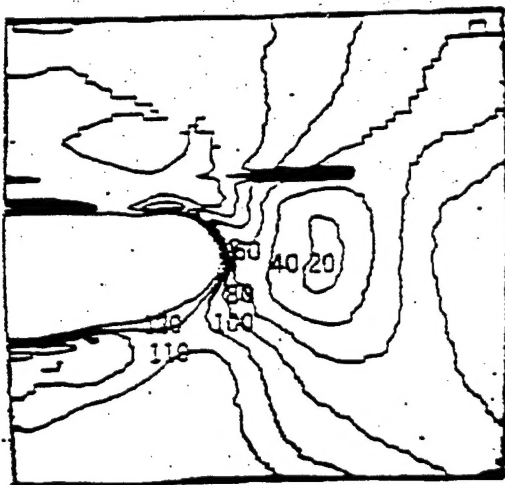


6% STRAIN

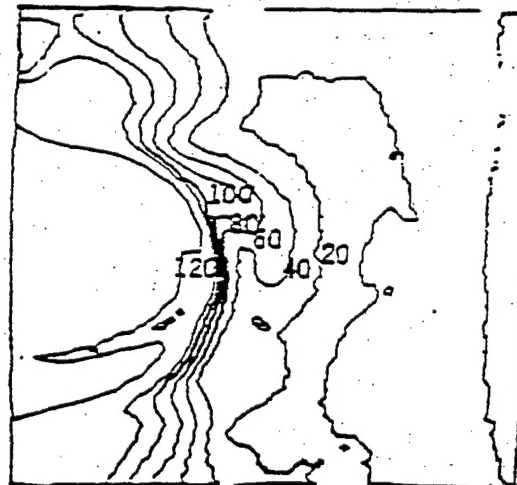


3% STRAIN

(a) unloading branch of the first strain cycle



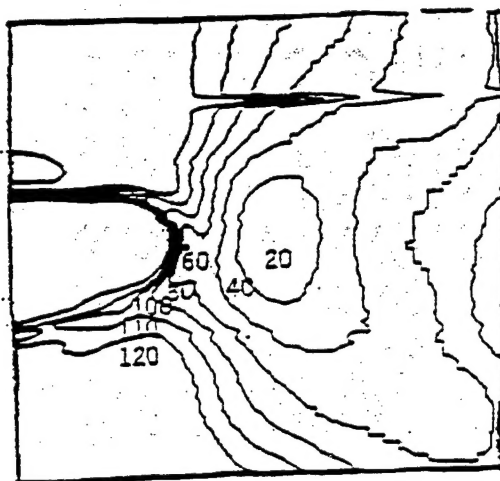
3% STRAIN



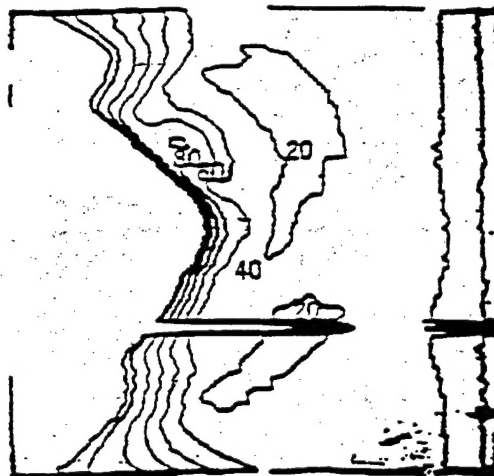
6% STRAIN

(b) loading branch of the second strain cycle

Fig. 6. Iso-intensity contour plots of acoustic images near the tip of the center crack (3% applied strain and 6% applied strain)



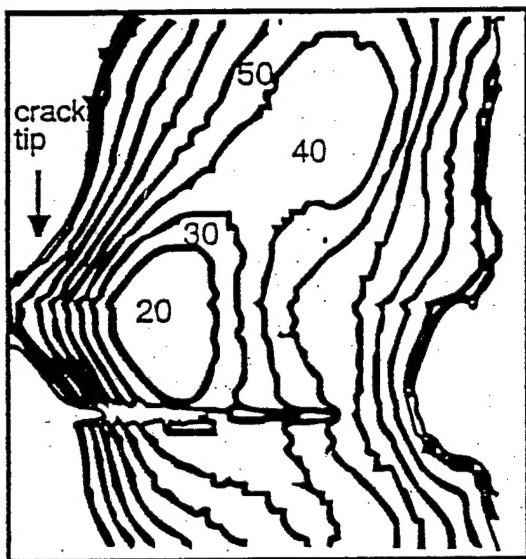
3% STRAIN



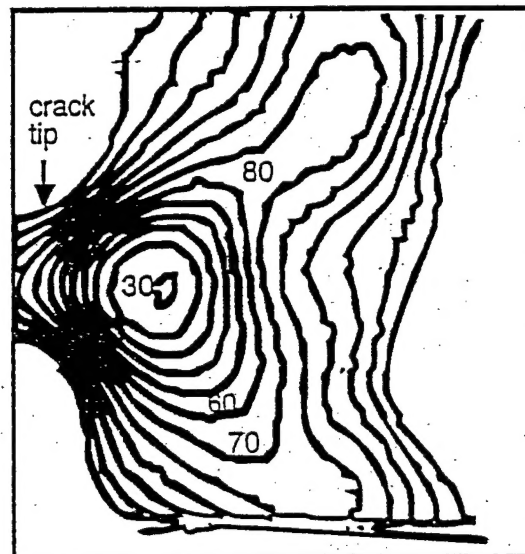
6% STRAIN

(c) loading branch of the third strain cycle

Fig. 6. Iso-intensity contour plots of acoustic images near the tip of the center crack (3% applied strain and 6% applied strain)

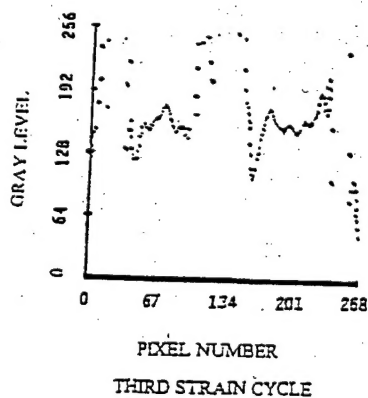
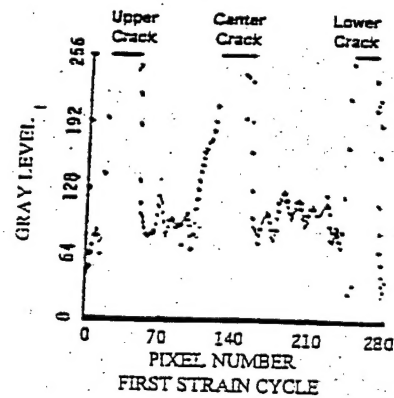
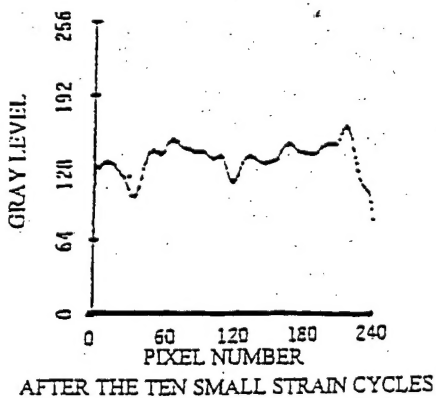
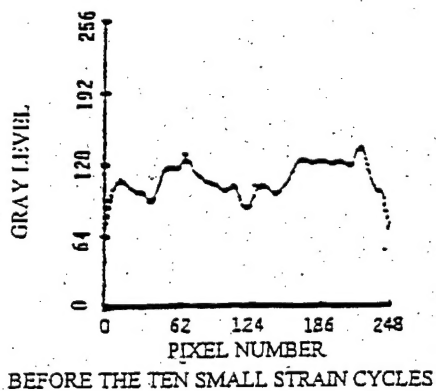
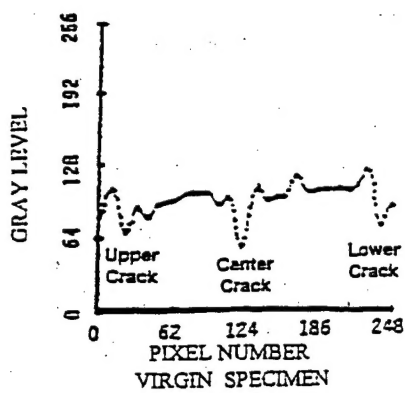


(a) before the 10 small strain cycles



(b) after the 10 small strain cycles

Fig. 7. Iso-intensity contour plots of acoustic image near the tip of the center crack at 0% applied strain



(a) 0% applied strain

(b) 6% applied strain

Fig. 8. Profile plots of the intensity of the transmitted acoustic energy I_t along the specimen's vertical plane of symmetry